

Article

Site Response Evaluation in the Trans-Mexican Volcanic Belt Based on HVSr from Ambient Noise and Regional Seismicity

L. Francisco Pérez-Moreno ¹, Quetzalcoatl Rodríguez-Pérez ^{2,*}, F. Ramón Zúñiga ³, Jaime Horta-Rangel ¹, M. de la Luz Pérez-Rea ¹ and Miguel A. Pérez-Lara ¹

¹ Facultad de Ingeniería, Universidad Autónoma de Querétaro, Querétaro 76010, Mexico; lf.perezm@uaq.mx (L.F.P.-M.); horta@uaq.mx (J.H.-R.); perea@uaq.mx (M.d.l.L.P.-R.); migperez@uaq.mx (M.A.P.-L.)

² Consejo Nacional de Ciencia y Tecnología, Dirección Adjunta de Desarrollo Científico, Ciudad de México 03940, Mexico

³ Centro de Geociencias, Universidad Nacional Autónoma de México, Querétaro 76230, Mexico; ramon@geociencias.unam.mx

* Correspondence: quetza@geociencias.unam.mx

Featured Application: The results obtained in this study allow an initial overview of the variation of the site response in an area for which low to moderate seismic risk is usually considered. The information presented may be used to analyze the seismic effects in the study zone associated with the geological characteristics.



Citation: Pérez-Moreno, L.F.; Rodríguez-Pérez, Q.; Zúñiga, F.R.; Horta-Rangel, J.; Pérez-Rea, M.d.l.L.; Pérez-Lara, M.A. Site Response Evaluation in the Trans-Mexican Volcanic Belt Based on HVSr from Ambient Noise and Regional Seismicity. *Appl. Sci.* **2021**, *11*, 6126. <https://doi.org/10.3390/app11136126>

Academic Editors: Miguel Llorente Isidro, David Moncoulon, Ricardo Castedo and Filippos Vallianatos

Received: 28 April 2021

Accepted: 28 June 2021

Published: 30 June 2021

Publisher's Note: MDPI stays neutral with regard to jurisdictional claims in published maps and institutional affiliations.



Copyright: © 2020 by the authors. Licensee MDPI, Basel, Switzerland. This article is an open access article distributed under the terms and conditions of the Creative Commons Attribution (CC BY) license (<https://creativecommons.org/licenses/by/4.0/>).

Abstract: The Trans-Mexican Volcanic Belt (TMVB), located in central Mexico, is an area for which low to moderate seismic risk is considered. This is based on the limited instrumental data available, even though large historical earthquakes have damaged some urban centers in the past. However, site effects is an aspect that must be considered in estimating risk, because there are some instances of important amplifications that have been documented with serious effects. In this work, ambient noise and earthquake records from 90 seismic permanent and temporary stations are used to analyze site response in the TMVB. The results obtained show a heterogeneous range in the value of the fundamental frequency. When possible, a comparison was made of the results obtained from ambient noise and earthquake records. In almost all these comparisons, no significant differences were observed in terms of the fundamental frequency. However, there were some stations with a flat average HVSr ambient noise curve that contradicted earthquake data results, which showed peaks at some frequencies. Our results are a first step towards categorizing the different site responses in the TMVB but in order to provide finer details, it is necessary to improve the actual monitoring conditions.

Keywords: site effects; spectral ratio; trans-mexican volcanic belt

1. Introduction

Within the context of seismic engineering, the study of site response involves changes in variables related to the seismic intensity, in terms of amplitude, duration, and frequency content. These changes depend on the geological features at the measurement site, and usually, lead to larger amplitudes on soil sites than on hard rock.

Throughout history it is possible to find documented cases in which site effects have played a decisive role in observed damage after significant earthquakes, such as in San Francisco (1906), Mexico City (1985 and 2017), and Kobe (1995). Thus, in the seismic design of buildings and civil infrastructure it is important to estimate the maximum expected intensities at the site.

The evaluation of changes in amplitude of ground motion of a particular site is commonly made with respect to a reference position. The most popular and reliable way to do this is through the Standard Spectral Ratio (SSR) technique [1]. This method is based

on the ratio of the Fourier amplitude spectra observed during an earthquake at soil $A_i(f)$ to reference site $A_j(f)$. The Fourier spectra of ground motion $A(f)$ can be expressed as the multiplication of source $S(f)$, path $P(f)$, and site $H(f)$ terms in the frequency domain:

$$A(f) = S(f) \times P(f) \times H(f) \quad (1)$$

where f is the frequency.

In the SSR technique, the reference site is required to have the most homogeneous geological conditions as it is assumed to be free of anomalous amplifications. The two sites should be close to each other in comparison with the distance to the source. Considering that the analysis is performed for stations which register the same earthquake:

$$SSR(f) = \frac{|A_i(f)|}{|A_j(f)|} = \frac{|H_i(f)|}{|H_j(f)|}. \quad (2)$$

However, it is not always possible to find records of the same event with a good signal-to-noise (S/R) ratio in two stations that meet these conditions. Thus, the Horizontal-to-Vertical Spectral Ratio (HVSr) technique [2] is used as an alternative to studying the site response. In this method, the ratio between the mean of the horizontal components $A_{Hi}(f)$ and the vertical component $A_{Vi}(f)$, recorded in a single station, is calculated:

$$HVSr(f) = \frac{|A_{Hi}(f)|}{|A_{Vi}(f)|}. \quad (3)$$

This technique can be used to estimate the fundamental resonant frequency (f_0) of a site, but is unreliable for determining its transfer function [3].

In the literature, several studies can be found in which the site response is analyzed in areas around the world, based on these empirical techniques and numerical models [4–8]. The study of this phenomenon remains current and it is an important issue to be considered in the estimation of seismic risk and damage prevention, even in areas of low seismicity [9].

The Trans-Mexican Volcanic Belt (TMVB), located in central Mexico (Figure 1), is an example of those areas where the site response might represent a potential risk despite the low frequency of earthquakes. It is a volcanic arc that covers Cretaceous and Cenozoic magmatic provinces [10]. Seismicity in this region is related to extensional faults in the crust and normal faults in the subducted Cocos plate. This zone is located between $18^{\circ}30'$ and $21^{\circ}30'$, and extends from the coast of the Pacific Ocean to the Gulf of Mexico. It has an approximate length of 1000 km and a variable width of 90–230 km.

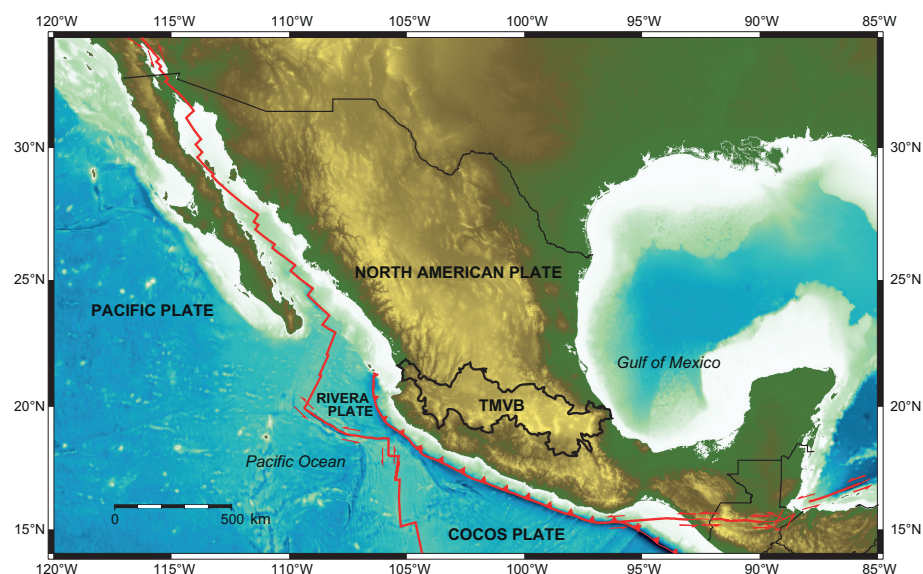


Figure 1. Location of the Trans-Mexican Volcanic Belt and interaction of tectonic plates in Mexico.

This area presents low seismicity, compared to the Pacific Ocean coast, where the Cocos plate subducts under the North American plate. Nevertheless, there are important recent and historical occurrences of destructive events [11,12]. Examples of these is the earthquake that occurred in Acambay on 12 November 1912 (Mw 6.9, H = 33 km) [13], and more recently in Puebla on 19 September 2017 (Mw 7.1, H = 51.2 km) [14]. This aspect is particularly important, in view that the TMVB comprises some of the largest cities in Mexico with significant industrial development and population growth in the last years.

It may be difficult to find a zone in the TMVB with negligible site effects, due to the variability in geological properties [10]. Several articles have been published on this topic related to Mexico, mainly focused on the behavior of site effects in Mexico City.

Ordaz et al. [15] found that stations located in the hill zone in the Valley of Mexico present amplifications that are 10 times higher than those predicted from ground motion attenuation equations. In a later study, García et al. [16] compared amplification responses at some of the stations analyzed by [15]. The records analyzed corresponded to inslab earthquakes with an epicenter outside the TMVB, and they observed similar behavior despite the source type and location.

Singh et al. [17] briefly discuss HVSr curves for 2 stations crossing the TMVB, obtained from records of 9 shallow coastal earthquakes on the Pacific Ocean coast. Likewise, Lozano et al. [18] studied the influence of source characteristics on the site effects in the Valley of Mexico from 36 interplate and inslab Mexican earthquakes and 12 teleseismic events originated in South America. Their results agree with those obtained by [16] and concluded that observed site effects were independent of the characteristics and location of the source.

Clemente-Chávez et al. [19] presented the first study of site effects in the TMVB outside the Valley of Mexico, based on local shallow seismicity. They analyzed HVSr curves obtained from 22 earthquakes recorded by 25 seismological stations located in the study zone. The events studied have depths $H < 10$ km, and magnitudes between 3.6 and 4.3. Average values for the fundamental frequency f_0 and amplification factors obtained from the HVSr curves were reported. Their results were compared with previous studies and they attributed the differences found to the location of the source. However, due to the limited amount of data employed, some of their conclusions were supported only with one or two records. Furthermore, it should be considered that HVSr curves do not unequivocally represent the actual site amplification.

Considering the low density of permanent seismological stations in the TMVB [20], the number of records that can be analyzed with the SSR technique is very limited. So, the use of ambient noise records represents a feasible option to include additional data for the analysis of site response in terms of f_0 . In this paper, we analyze HVSr curves obtained from ambient noise and regional instrumental records related to 121 crustal and inslab events with an epicenter inside the TMVB. Data considered were recorded by 90 seismological stations belonging to seven seismic networks.

The results of our study may be useful in disaster prevention and in estimating the behavior of future buildings in the study area. The information presented may also be used to complement studies examining the damage observed to existing infrastructure after the occurrence of a seismic event [21,22]. However, it is important to consider that a more accurate and reliable analysis can be carried out throughout microzonation studies, so our results only give a general overview.

2. Data and Methods

To perform this study, we compiled a catalog of earthquakes with epicenter inside the area of the TMVB, based on the seismicity catalogs of the Servicio Sismológico Nacional [23], the U.S. Geological Survey [24], and the International Seismological Centre (ISC) [25]. Avoiding duplications and magnitudes reported as “non-calculable”, 2113 earthquakes with magnitude 1.5–7.8 and depth 1–191 km, were selected.

Based on this information, instrumental records were searched in seven permanent and temporary seismological networks in Mexico (Table 1), with broadband stations located inside the TMVB. It should be considered that over time there have been significant changes in instrumental density in this zone [20]. Additionally, the stations that belong to permanent networks are widely dispersed, and the availability of continuous data is limited to the last 30 years.

Table 1. Seismological networks that were analyzed in this study. The continuous data availability is variable depending on each station.

Network	Period
SSN	2002–present
CGEO	2003–present
GEOSCOPE	1990–present
MASE	2004–2007
CODEX	2006–2008
MARS	2006–2007
GECO	2013–2018

Data were gathered from stations with velocity sensors belonging to Servicio Sismológico Nacional (SSN) [23], Centro de Geociencias de la Universidad Nacional Autónoma de México (CGEO), GEOSCOPE [26], and the temporary networks: The MesoAmerican Subduction Experiment (MASE) [27,28], Colima Deep Seismic Experiment (CODEX) [29], Mapping the Rivera Subduction Zone (MARS) [30], and Geometry of the Cocos Plate (GECO) [31].

The stations belonging to SSN and CGEO are equipped with STS-2 broadband seismometers with sampling rates of 80 and 100 Hz. Only the ACIG station has a Trillium 120 seismometer with a sampling rate of 20 Hz. In the case of the GEOSCOPE network, the UNM station has a velocity sensor STS-1 20 samples/s. During their period of operation, the GECO network stations were equipped with Reftek 151B-60 and Guralp 40T sensors. The temporary networks MASE and CODEX had CMG 3T, and 40T seismometers, respectively, with a sampling rate of 100 Hz. The MARS network was equipped with CMG 3T sensors of 40 sps.

Only records that met the following criteria were considered for the analyses: (1) Station and epicenter located inside the TMVB; (2) signal-to-noise ratio (S/R) > 2.0; and (3) clear arrival of P and S waves, based on visual inspection.

Considering these restrictions, a total of 352 records related to 24 inslab and 97 crustal earthquakes were chosen (Figure 2). Such events have magnitudes between 2.0 and 7.1, a hypocentral depth of $1 \leq H \leq 105$ km, and occurred between 1993 and 2019 in the TMVB. The main characteristics of the selected earthquakes are listed in Table 2.

In Figure 2 it can be observed that in the central zone there is the lowest number of records. As mentioned by Zúñiga et al. [20], the other regions present higher seismic activity due to active fault systems, the subduction zone on the Pacific Ocean coast, and the occurrence of inslab earthquakes in the central-eastern sector.

The number of records selected for each station was variable, and in most of them, the data with the characteristics sought was considerably limited. An HVSR analysis was performed at all stations with at least 10 earthquake records. This threshold was considered to include as many stations as possible, trying not to compromise the reliability of the results. It is important to note that despite the large number of seismological stations belonging to MASE, MARS, and CODEX networks, the suitable records were limited due to the characteristics of the earthquakes during their short period of operation.

The processing of records was performed by means of the package Geopsy [32]. For each analyzed record, the mean and the trend were removed. The corresponding Fourier Acceleration Spectra (FAS) were smoothed using the Konno–Omachi function [33],

considering a b-value of 20. Window lengths that included 95% of the total energy were taken, beginning from the S-wave arrival.

Table 2. A database of crustal and inslab earthquakes with records that met the considered criteria. The value of magnitude is the one reported by SSN.

Date dd/mm/yyyy	Origin Time hh:mm:ss	Magnitude	Depth (km)	Latitude (°)	Longitude (°)
08/03/1993	14:37:41	3.3	11	19.25	−98.93
02/11/1994	15:31:21	3.7	7	19.41	−98.90
27/03/1996	08:05:15	3.4	8	19.77	−99.01
17/04/1996	11:19:10	3.5	10	19.21	−98.94
06/09/1996	06:55:00	4.0	5	19.21	−98.36
03/07/1997	19:39:32	2.8	7	19.25	−99.44
25/12/1997	01:29:10	4.1	11	18.97	−98.59
15/03/1998	02:01:49	4.2	5	19.50	−100.26
26/10/1998	02:35:10	3.0	6	19.06	−99.17
26/10/1998	07:50:06	3.3	4	19.06	−99.20
31/12/1998	06:44:05	3.8	2	18.98	−98.65
04/01/1999	23:21:59	3.5	3	20.11	−98.98
19/05/1999	20:23:06	3.1	5	19.19	−98.96
22/05/1999	06:57:26	3.1	4	19.18	−98.97
07/06/1999	00:24:14	3.3	5	19.17	−98.96
15/06/1999	20:42:04	7.0	63	18.13	−97.54
20/06/1999	10:25:21	4.0	3	19.31	−98.48
07/12/1999	13:53:49	3.4	3	19.22	−98.92
04/03/2000	20:55:23	4.1	4	18.84	−98.57
12/03/2000	03:44:48	4.1	5	20.10	−99.29
06/07/2000	08:36:24	3.3	8	19.18	−98.93
06/07/2000	13:15:34	3.4	5	19.19	−98.96
21/07/2000	06:13:39	6.0	48	18.09	−98.97
14/10/2000	02:44:48	3.1	12	19.36	−99.19
15/10/2000	07:50:43	2.7	5	19.39	−99.11
01/03/2001	16:26:42	3.5	46	18.98	−99.82
13/06/2001	03:57:43	3.2	12	19.27	−99.42
14/09/2001	17:13:15	2.9	14	19.31	−99.30
15/11/2001	22:18:22	3.5	4	19.56	−99.16
09/05/2002	14:25:43	3.7	19	19.49	−99.01
04/02/2003	10:59:03	4.1	2	18.92	−98.51
15/12/2003	10:39:38	4.0	4	20.35	−99.07
13/09/2004	20:58:34	3.1	11	19.42	−99.17
16/04/2005	22:55:25	3.8	16	19.43	−99.00
12/05/2005	08:06:25	3.4	37	19.20	−98.97
07/08/2005	03:25:09	4.0	7	19.74	−98.61
16/10/2005	14:12:36	3.5	14	19.30	−99.20
23/11/2005	23:11:26	3.6	20	19.35	−98.94
24/01/2006	12:59:38	3.7	5	20.34	−99.22
28/02/2006	23:58:49	3.4	2	19.35	−99.02
12/03/2006	01:41:32	3.6	2	19.17	−98.95
12/03/2006	01:47:21	3.4	5	19.18	−98.96
05/05/2006	15:24:06	3.5	1	19.17	−98.95
27/06/2006	15:40:10	4.0	16	19.26	−102.32
14/07/2006	05:15:28	3.7	72	20.19	−98.87
18/12/2006	03:38:31	3.9	44	20.92	−104.47
25/01/2007	14:38:22	3.7	30	19.18	−99.16
30/01/2007	19:00:10	3.7	9	20.35	−103.87
14/05/2007	08:23:27	4.4	12	21.36	−104.75
30/05/2007	20:42:28	4.0	3	19.21	−99.45
22/06/2007	13:36:52	4.2	25	19.16	−96.96
20/10/2007	19:25:54	3.7	75	19.47	−102.20
20/10/2007	02:37:27	3.9	20	19.95	−101.97
21/10/2007	11:29:53	3.7	93	19.53	−102.17
23/03/2009	02:53:36	3.9	46	18.92	−97.01
22/05/2009	19:24:18	5.7	62	18.11	−98.46
29/11/2009	06:34:12	4.0	5	19.35	−103.76
17/04/2010	07:03:29	4.0	2	20.45	−99.04

Table 2. Cont.

Date dd/mm/yyyy	Origin Time hh:mm:ss	Magnitude	Depth (km)	Latitude (°)	Longitude (°)
18/04/2010	18:26:25	4.0	79	19.27	−97.46
18/05/2010	05:29:09	4.0	5	20.35	−98.92
18/05/2010	05:32:37	3.4	10	20.37	−98.96
03/10/2010	23:07:11	4.0	6	19.48	−103.52
19/12/2010	02:46:45	4.1	16	19.03	−97.21
28/09/2011	10:51:18	4.1	23	19.76	−96.64
18/05/2012	03:07:58	4.4	1.6	20.26	−103.44
05/10/2012	00:14:57	4.2	16.1	19.45	−102.26
08/02/2013	01:24:58	3.8	6.5	20.12	−100.48
21/06/2013	09:41:33	4.0	2	18.52	−98.74
18/09/2013	00:26:15	3.3	5	19.62	−96.79
14/12/2013	22:33:40	4.1	104.6	19.45	−103.71
24/12/2013	15:27:07	3.6	3	19.52	−103.80
16/01/2014	07:23:57	3.4	9	19.27	−97.26
09/05/2014	07:50:49	3.7	3	18.98	−97.27
19/07/2014	11:57:23	3.5	8	19.17	−98.97
04/08/2014	21:10:03	4.0	59.2	18.18	−97.83
08/11/2014	02:46:50	3.6	5	19.51	−96.78
01/12/2014	08:50:06	3.4	2	19.35	−99.22
06/05/2015	04:06:46	3.7	10	19.16	−97.17
09/08/2015	15:17:17	3.7	5	18.96	−98.21
16/08/2015	14:29:17	3.4	20	19.65	−97.55
25/10/2015	02:52:43	3.7	77.3	19.26	−97.30
07/11/2015	02:29:50	4.1	5	19.73	−96.70
26/12/2015	14:08:36	4.0	5	19.55	−102.11
16/01/2016	06:28:46	3.1	42.6	19.65	−96.80
27/01/2016	21:22:44	4.1	69.5	18.28	−97.33
28/01/2016	11:41:49	3.4	44	19.45	−96.72
08/02/2016	21:16:07	4.6	6.9	19.66	−97.35
13/03/2016	19:13:50	3.7	55.3	19.31	−97.03
01/04/2016	22:34:33	3.7	58.6	18.27	−97.78
01/04/2016	05:06:51	3.1	5	19.63	−96.64
01/04/2016	05:39:39	3.4	4.1	19.68	−96.73
11/05/2016	22:35:20	4.8	8	20.81	−103.52
15/05/2016	01:43:48	3.9	5	20.82	−103.47
11/06/2016	19:06:14	3.9	12.5	18.85	−97.19
16/06/2016	00:56:29	3.3	10	19.95	−96.77
24/06/2016	00:22:54	3.4	20	19.23	−97.40
27/06/2016	19:12:25	3.4	10	19.95	−96.76
12/07/2016	17:33:29	3.5	5	20.77	−103.45
19/07/2016	04:34:43	3.9	56.7	18.29	−97.38
28/07/2016	18:21:06	3.9	5	20.73	−103.45
08/08/2016	15:57:08	3.8	20	19.44	−96.72
29/08/2016	16:24:17	3.8	3	18.95	−98.58
26/09/2016	03:44:44	3.6	10.1	19.51	−96.45
15/10/2016	01:51:48	4.1	51.3	18.87	−96.99
26/02/2017	02:11:29	4.0	23.7	19.88	−96.85
01/06/2017	13:36:59	3.8	5	19.24	−97.04
09/07/2017	09:03:33	3.5	30.7	19.69	−96.81
04/08/2017	01:07:36	3.5	10	19.50	−96.43
10/09/2017	02:54:12	2.7	9.4	19.31	−99.18
19/09/2017	18:14:40	7.1	51.2	18.33	−98.68
29/09/2017	17:02:23	3.8	50.7	18.35	−98.66
01/11/2017	20:48:04	4.3	52.8	18.25	−98.60
06/11/2017	09:38:09	3.1	3	19.19	−98.44
09/11/2017	10:12:07	2.0	8.5	19.38	−99.19
18/11/2017	07:21:54	3.6	32.4	18.64	−98.48
24/12/2017	12:25:12	3.4	3.1	18.82	−98.60
08/06/2018	18:09:34	3.9	11.5	19.95	−96.75
30/07/2018	22:15:54	3.9	24.6	19.27	−97.34
30/03/2019	22:09:22	3.9	5	19.44	−96.71
14/07/2019	19:37:06	3.8	37	19.21	−97.23
23/07/2019	19:03:20	4.0	32	19.27	−97.43

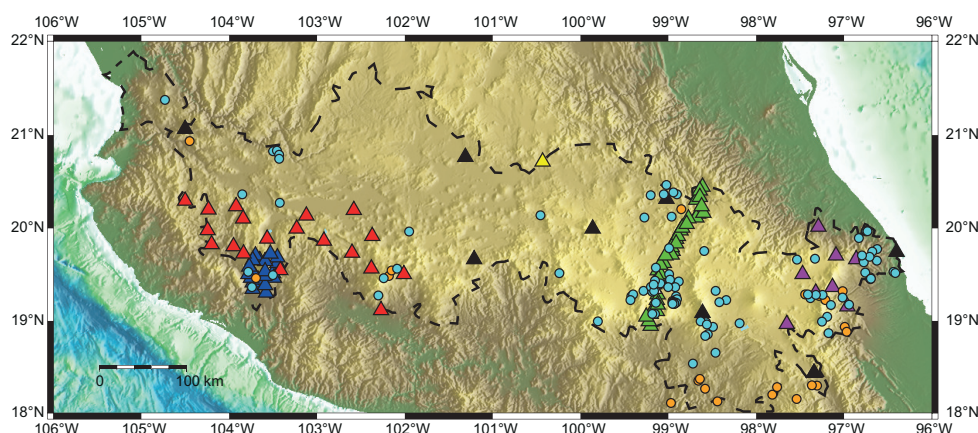


Figure 2. Location of epicenters and seismological stations analyzed in this study. Cyan circles: Crustal earthquakes; orange circles: Inslab earthquakes. Red triangles: MARS temporary network stations; blue triangles: CODEX temporary network stations; green triangles: MASE temporary network stations; purple triangles: GECO temporary network stations; black triangles: SSN permanent network stations; yellow triangle: CGEO permanent station; and white triangle: GEOSCOPE permanent station. Dashed line: TMVB.

Due to the lack of earthquake records, an HVSR analysis was performed in all the stations using ambient noise data. Although the energy of ambient noise does not compare with that of an earthquake, this second analysis allowed us to increase the number of stations analyzed and to compare the results obtained with both procedures. For each station, a database of 30 records of one-hour duration was collected on random dates within its period of operation. In all ambient noise records, the mean and trend were removed and the same smoothing process was applied as in the earthquake records. For the HVSR analyses, the records were divided into 60 windows of 1 min and the root mean square of the horizontal components was calculated. SESAME criteria [34] were considered for the analyses and classification of the curves obtained. Finally, the results were correlated with the geological characteristics of the study area.

3. Results

Due to the large extension of the study area, the stations analyzed were grouped into four zones. This division was based on the distribution of stations and on geologic information given by [10]. Most of the average curves shown correspond to the HVSR analyses based on ambient noise data, between 0.1 and 25 Hz. Some of the considered stations have a Nyquist frequency of 10 and 20 Hz, so not all curves are displayed in the same frequency range. When possible, a comparison is made with results from earthquake records. Regarding geology, information from the Geologic Map of North America [35] was used.

3.1. Western TMVB

In the westernmost part of the TMVB, there are three main fault systems: Tepic-Zacoalco, Colima, and Chapala [10]. Regarding significant earthquakes, there is a historical account of the occurrence of a damaging event during the 16th century near the town of Ameca, in the state of Jalisco. For this event, a magnitude $M_w 7.2 \pm 0.3$ was estimated from a rupture vs. magnitude scaling relation [36,37]. Another earthquake occurred on 2 October 1847, with a mean magnitude of 5.7 ± 0.4 which has been associated to the faults of the Chapala Graben. It affected several towns and produced important damages to buildings. An intensity of IX has been estimated for this event [38].

Later, on 11 February 1875 an earthquake near the city of Guadalajara caused great destruction in nearby areas including dozens of deaths [39].

Figure 3 shows the seismological stations analyzed in the Western sector of the TMVB. As can be observed, there is only one station belonging to a permanent seismological network. The other temporary stations are mostly concentrated in the south of this sector.

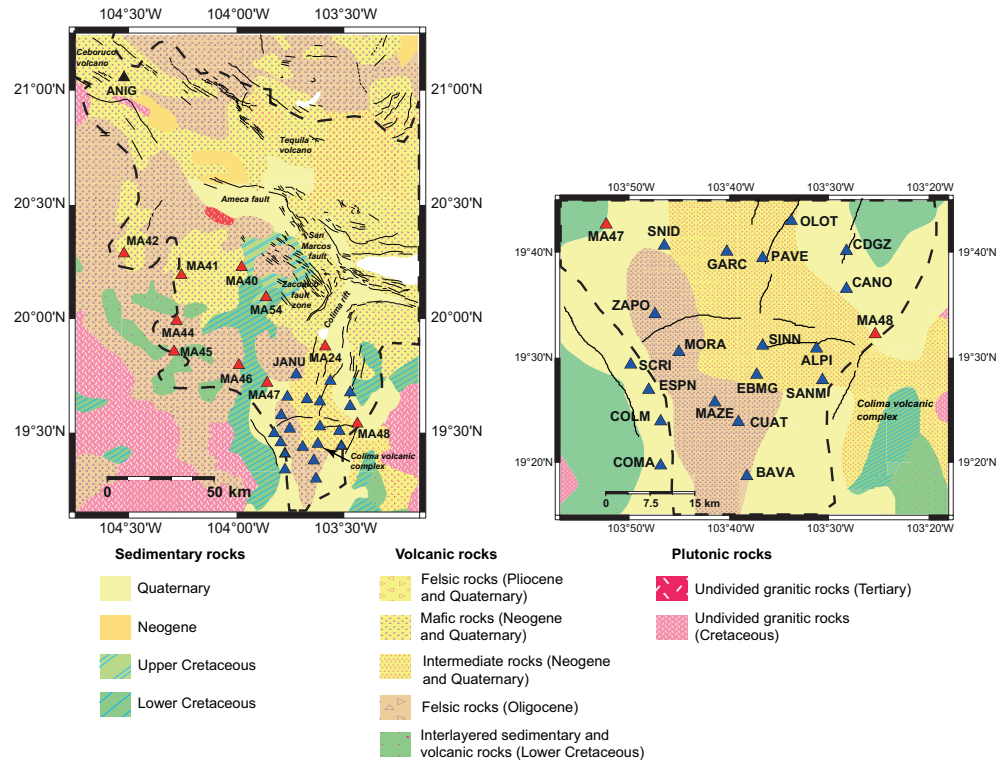


Figure 3. Geological units in the western sector of the TMVB [35]. Red triangles: MARS temporary network stations; blue triangles: CODEX temporary network stations; and black triangle: SSN permanent network station. Continuous line: Main fault systems in the area; dashed line: TMVB.

In this sector, there are a variety of geological formations ranging from the Lower Cretaceous to the Quaternary [35]. Most of the stations analyzed are located in the vicinity of the Colima volcanic complex. Figure 4 shows some of the average HVSr curves obtained in this zone, in which only the ANIG station could be analyzed with earthquake records.

In some curves there can be observed flat responses or complex shapes with low amplitudes at different frequencies: MA47, MORA, MAZE, CUAT, ZAPO, MA24, OLOT, SNID, SINN, EBMG (Figure 4), SCRI, and COMA (Figure 5). Station MA47 is located on sedimentary rocks from the Lower Cretaceous. Its HVSr curve has a flat shape and no significant impedance contrast is identified. In contrast, stations MORA, MAZE, CUAT, and ZAPO were deployed on Oligocene felsic rocks and near their location there are volcanic and sedimentary rocks from the Neogene and Quaternary. The site response could be attributed to lateral heterogeneity and the presence of sedimentary rocks from the Cretaceous. Stations MA24, OLOT, SINN, and EBMG were located on mafic and intermediate rocks from the Neogene and Quaternary. MA24 and OLOT were relatively close to each other, but a resonant frequency can not be identified in either of them. As for SINN and EBMG, the corresponding curves have a flat shape, indicating hard rock sites. Stations SCRI and COMA (Figure 5) were deployed on Quaternary sedimentary rocks, and in both of them a predominantly flat shape is also observed.

There is another group of stations in which the HVSr curves present multiple peaks, with amplitudes similar to what could be identified as the clearest peak. Station MA54 were located on sedimentary rocks from the Upper Cretaceous. The peak around 6 Hz could be attributed to a thin layer of sediments and the amplitude between 0.6 and 2 Hz to the contact with formations from the Lower Cretaceous. Meanwhile, MA46 were deployed on Oligocene felsic rocks. The observed peaks above 2 Hz could indicate multiple layers

of sediments of varying thickness above the bedrock. Station MA42 was on mafic and intermediate rocks from the Neogene and Quaternary. The shape of the HVSR curve corresponding to this station could be attributed to variations in the topography or a deep interface with Oligocene formations. SNID (Figure 4) and MA48 (Figure 5) were deployed on Quaternary sedimentary rocks. The amplitudes in SNID could be associated to lateral heterogeneities by means of its location near Neogene formations. Likewise, some of the multiple peaks in MA48 could be spurious or related to multiple layers of sediments at variable depth.

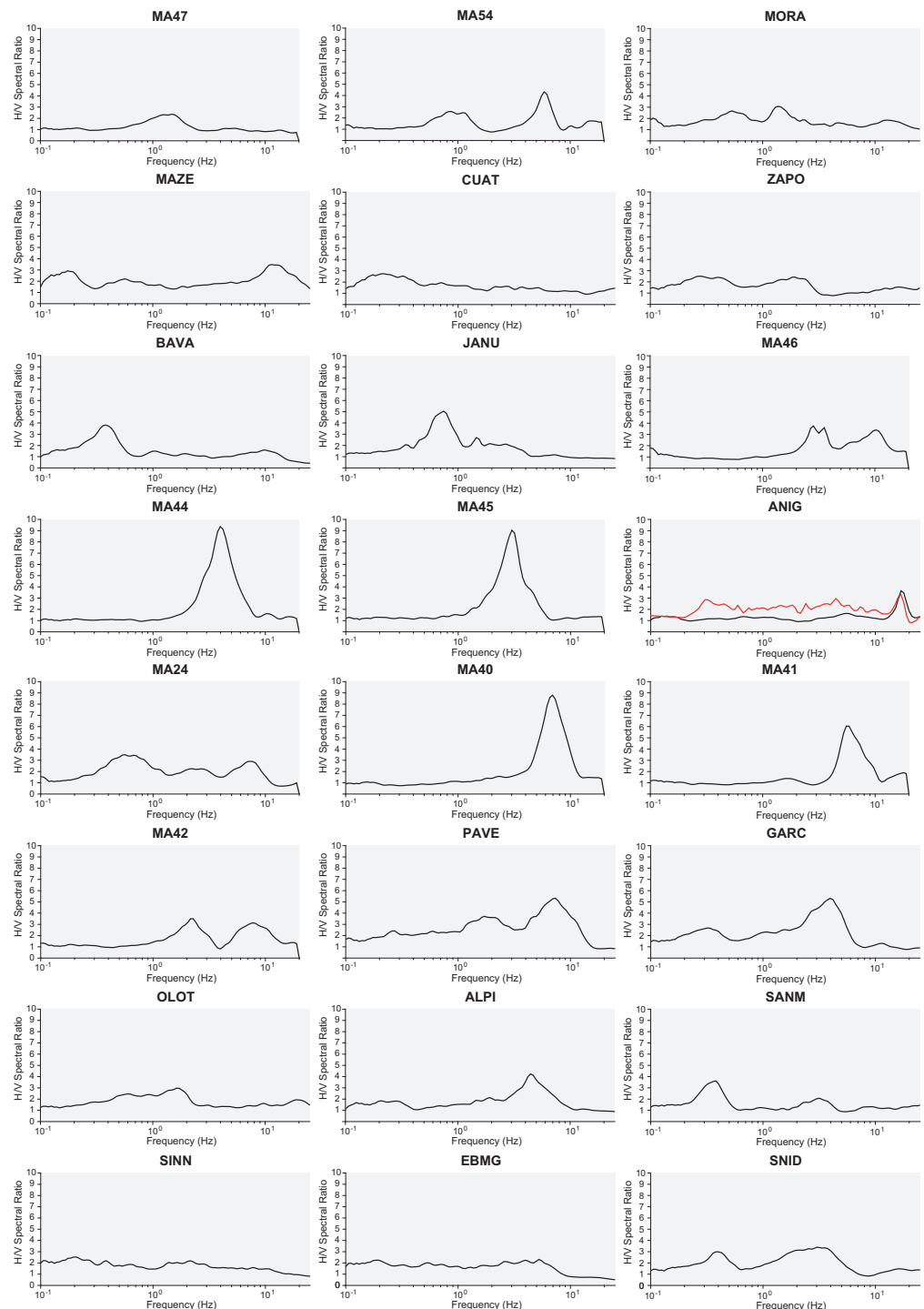


Figure 4. Average HVSR curves for stations located in the western sector of the TMVB. Blackline: HVSR results using ambient noise records; redline: HVSR results from earthquake records.

In the remaining stations, clear peaks of different amplitude can be observed, revealing different impedance contrasts between sediment layers and the bedrock: BAVA, JANU, MA44, MA45, ANIG, MA40, MA41, PAVE, GARC, ALPI, SANM (Figure 4), CDGZ, COLM, CANO, and ESPN (Figure 5). This is also indicative of possible amplifications in ground motion during the occurrence of seismic events. In the case of stations BAVA and JANU, located on Oligocene felsic rocks, the observed peaks at low frequencies could be associated to thick sedimentary deposits. High clear peaks at 3 and 4 Hz are observed at stations MA44 and MA45. These may be produced by strong impedance contrasts with interlayered sedimentary and volcanic rocks from the Lower Cretaceous.

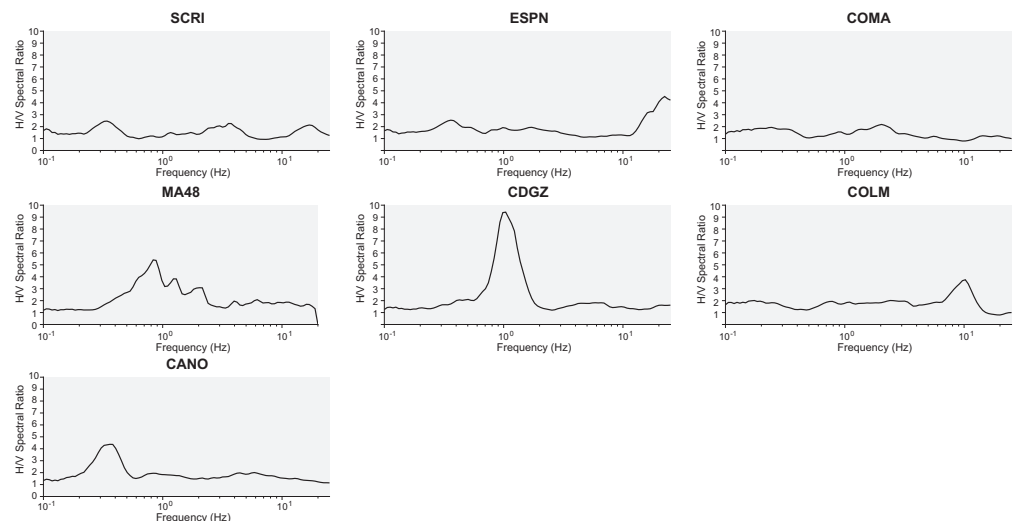


Figure 5. Average HVSR curves for stations located in the western sector of the TMVB.

The stations located on mafic and intermediate rocks from the Neogene and Quaternary have a heterogeneous response (ANIG, MA40, MA41, PAVE, GARC, ALPI, and SANM) (Figure 4). In general, a clear peak is observed above 5 Hz, which could be attributed to impedance contrast with thin layers of sediment. It should be noted that the average HVSR curve obtained with earthquake data at ANIG station does not vary significantly in its shape to that obtained from ambient noise. There is a peak above 10 Hz that could have been produced by the presence of thin volcanic layers.

Regarding the average HVSR curves of stations on Quaternary sedimentary rocks (ESPN, CDGZ, COLM, and CANO) there are varied shapes (Figure 5). In ESPN, there is a peak above 10 Hz which may require the analysis of a wider frequency bandwidth. The clear peak in CANO could be associated to contact with Neogene and Quaternary rocks. As for CDGZ, there is a high peak near 1 Hz, attributable to impedance contrast with layers of the Lower Cretaceous or thick layers of sediments. Likewise, in COLM there is a small peak around 10 Hz, probably due to the presence of shallow unconsolidated sediments.

3.2. Central TMVB

The Central sector is the one with the lowest instrumental density. There is a group of nine temporary stations concentrated on the southwest of the sector, and only two permanent stations that are considerably separated in the east (Figure 6). There were few earthquake records that met the established restrictions. For this reason, the results presented here only correspond to the analysis of ambient noise data.

Most of the stations in this sector were deployed on Neogene and Quaternary mafic rocks. In MA15, MA18, MA27, MA29, and MOIG, there are HVSR curves with flat shapes and no significant impedance contrast is observed, while stations MA20 and MA28 do not have clear peaks (Figure 7).

Station MA21 has a clear peak at 1 Hz and additional unclear peaks above this frequency. In this case, the shape of the HVSR curve could be related to the calderas

that predominate in the area or lateral variations with sedimentary rocks from the Lower Cretaceous. Furthermore, the curve corresponding to the IGIG station shows peaks at frequencies beyond 10 Hz. This permanent station is located on Felsic rocks from Neogene, and its response could be related to thin layers of sediments.

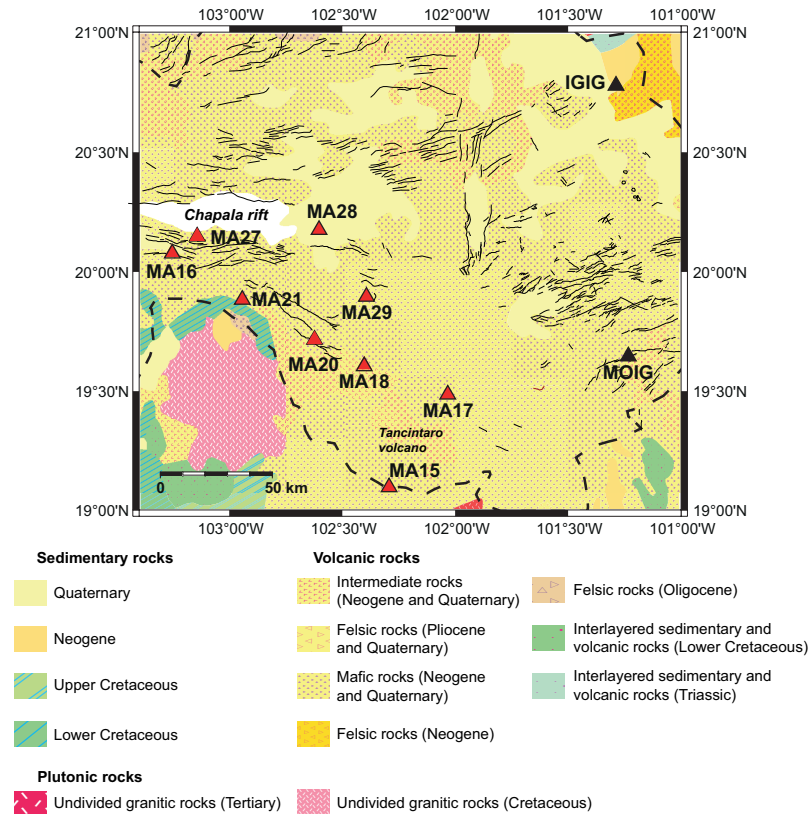


Figure 6. Geological units in the central sector of the TMVB [35]. Red triangles: MARS temporary network stations; black triangles: SSN permanent network stations. Continuous line: Main fault systems in the area; dashed line: TMVB.

In stations MA16 and MA17, there are clear peaks at 1.5 and 5 Hz, respectively. This could be attributed to impedance contrasts with layers of sediments of different thickness.

3.3. Central-Eastern TMVB

In the central-eastern zone of the TMVB is the Acambay fault system, covering some faults considered as active [40]. In the same area, there are the Taxco-San Miguel de Allende and Chapala-Tula systems, with evidence of activity in recent years. In this sector, a large number of relevant earthquakes can be mentioned over time, highlighting the following.

In the 18th century, there are reports of crustal earthquakes related to the Venta de Bravo fault. The first occurred in November 1734, followed by more than 30 strong and small events between November 1734 and March 1735 [39]. The largest crustal earthquake in the TMVB during the 20th century took place on 12 November 1912, in Acambay [13]. It had a magnitude of Mw 6.9 with a maximum intensity of IX in the epicentral area. Then, a series of 90 earthquakes were registered between February and June 1979 in a region comprising Maravatio and Mexico state. The mainshock occurred on 22 February 1979 with a magnitude Mw 5.3 and maximum intensity of VIII [40].

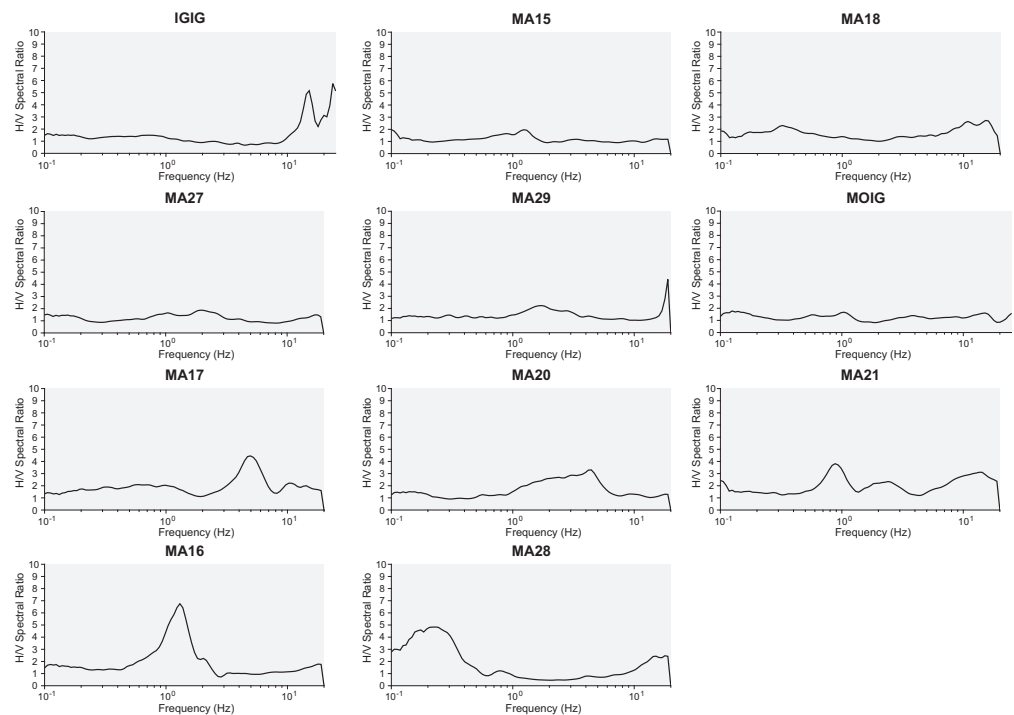


Figure 7. Average HVSR curves for stations located in the central sector of the TMVB.

Figure 8 shows the seismological stations analyzed in this sector. In this case, it was possible to analyze nine stations with earthquake data and to compare the results with the use of ambient noise. Particularly noteworthy are the stations belonging to the MASE temporary network, deployed between 2004 and 2007. Despite being numerous, due to the characteristics of the events that occurred during this period, only a few stations had earthquake records with the characteristics sought.

In this sector, there are some stations located on Neogene and Quaternary geological units (Figure 8). In JRQG, ECID, SNLU, COAC, PTRP, ESTA, and MIXC there are mostly flat HVSR curves, and no clear peaks are identified. In DHIG, CUIG, UNM, SABI, and PSIQ, the shape of the average curves obtained from ambient noise and earthquake records do not vary significantly (Figure 9). Small peaks can be observed at different frequencies that show no significant impedance contrasts or possible amplifications. As a result of this, the locations of these stations and those mentioned above may be considered as hard rock sites. In the HVSR curve corresponding to station TEPE (Figure 10), it is not possible to point out some value as the resonance frequency. This shape could be produced by lateral heterogeneity due to the vicinity of some Quaternary mafic rocks.

In some stations located on Quaternary volcanic rocks, there are almost HVSR curves of a flat shape (ACIG, PACH, MIMO, SAPE, SAPA, and TOSU). On the other hand, stations CUCE and CUNO have HVSR curves in which it is not possible to clearly identify any resonant frequency and could be considered as flat (Figure 10).

In station SALU, deployed on Quaternary sedimentary rocks, there are multiple peaks below 1 Hz and between 3 and 10 Hz (Figure 9). This could be due to the influence of topography or underlying geological units. The curve corresponding to station CHIC, located on Quaternary volcanic rocks, has multiple peaks at high frequencies, but only the one at 20 Hz can be considered as clear, indicating shallow layers of sediments. Additionally, in stations VEGU, ARBO, and VLAD, there are not very well-defined peaks between 1 and 10 Hz (Figure 10). These could be attributed to small impedance contrasts at different depths or lateral heterogeneity due to the presence of Neogene sedimentary rocks.

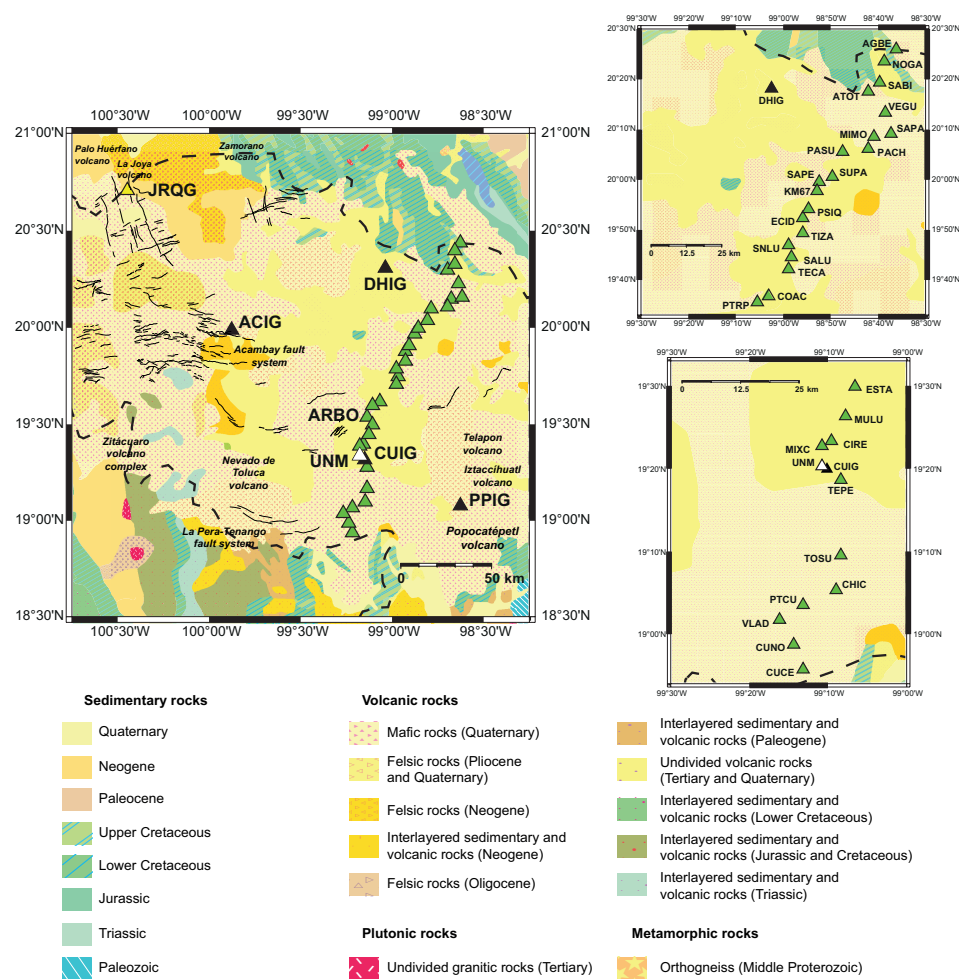


Figure 8. Geological units in the central-eastern sector of the TMVB [35]. Green triangles: MASE temporary network stations; black triangles: SSN permanent network stations; yellow triangle: CGEO permanent station; and white triangle: GEOSCOPE permanent station. Continuous line: Main fault systems in the area; dashed line: TMVB.

There are some stations in which clear peaks of varied amplitude can be identified. In the stations TECA, TIZA, and PASU, located on Quaternary sedimentary rocks, there are small peaks of a wide shape but low amplitude (Figure 9). This could indicate the presence of deposits of different stiffness and width, which by consolidation time have no significant contrasts with the underlying bedrock. The MULU and CIRE stations are special cases since the average HVSR curves present very high peaks at frequencies below 1 Hz. These responses can be explained by the fact that these temporary stations were located in the lakebed zone of Mexico City. In this area, there are reports of devastating effects during the earthquakes of 1985 and 2017.

At some of the remaining stations deployed on Quaternary volcanic rocks, it was possible to perform the analyses with ambient noise and earthquake data (NOGA, AGBE, KM67, and PPIG). The shape of the average HVSR curves obtained did not differ significantly and the amplitude only increased when earthquake records were used (Figure 10). A particularly special case is that of station KM67, where the HVSR curve obtained using ambient noise data is flat. However, when doing analysis with earthquake data, a clear peak is observed, revealing a significant impedance contrast. At this site, the energy associated with the seismic movement may have produced reverberations in underlying Cretaceous layers. In the case of the PPIG station, located at the Popocatepetl volcano, there is a peak above 10 Hz using ambient noise and earthquake data. Likewise, a peak below 1 Hz can be observed in the analysis with earthquake records. In ATOT, SUPA, and

PTCU there are clear peaks between 1 and 3 Hz that may be due to impedance contrasts with Cretaceous layers.

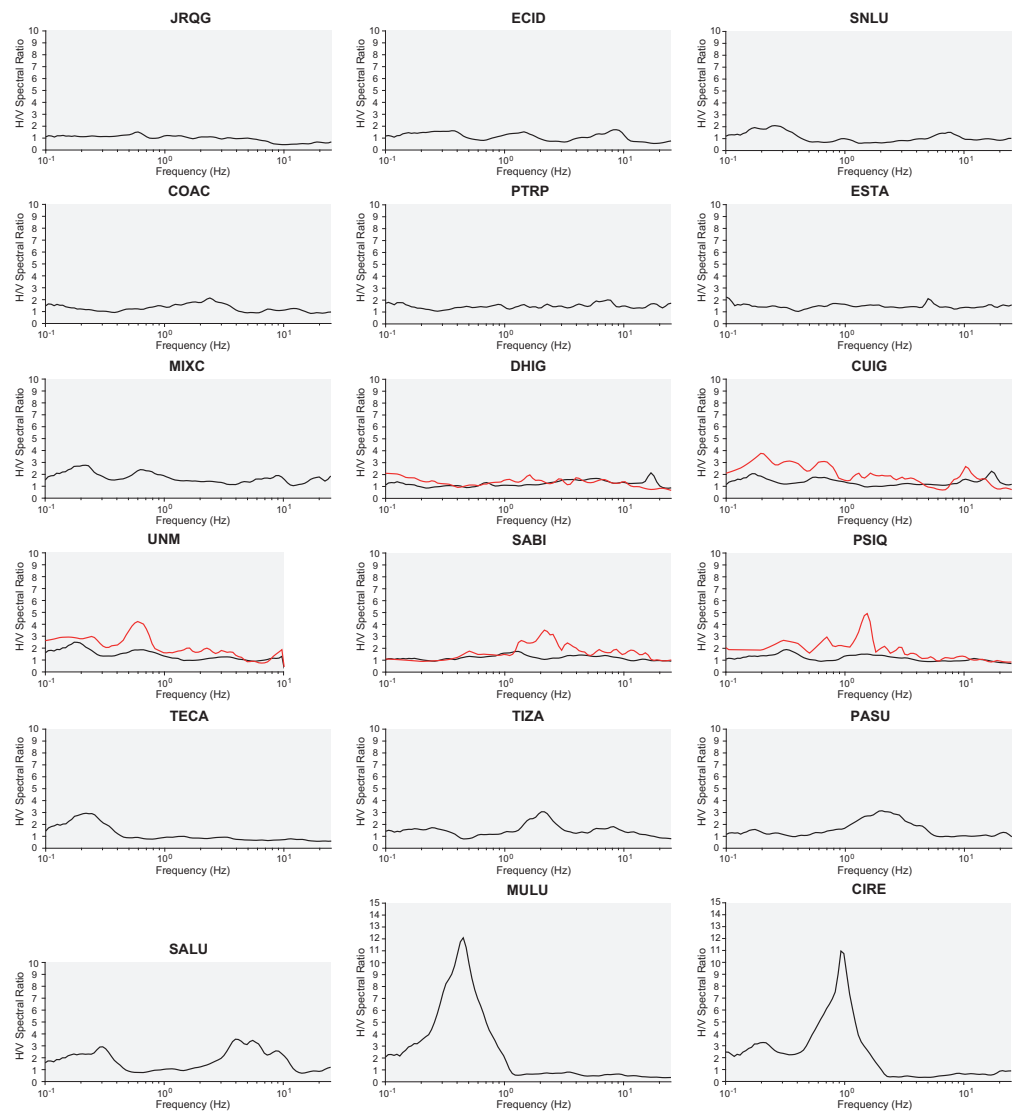


Figure 9. Average HVSR curves for some stations located in the central-eastern sector of the TMVB. Blackline: HVSR results using ambient noise records; redline: HVSR results using earthquake records.

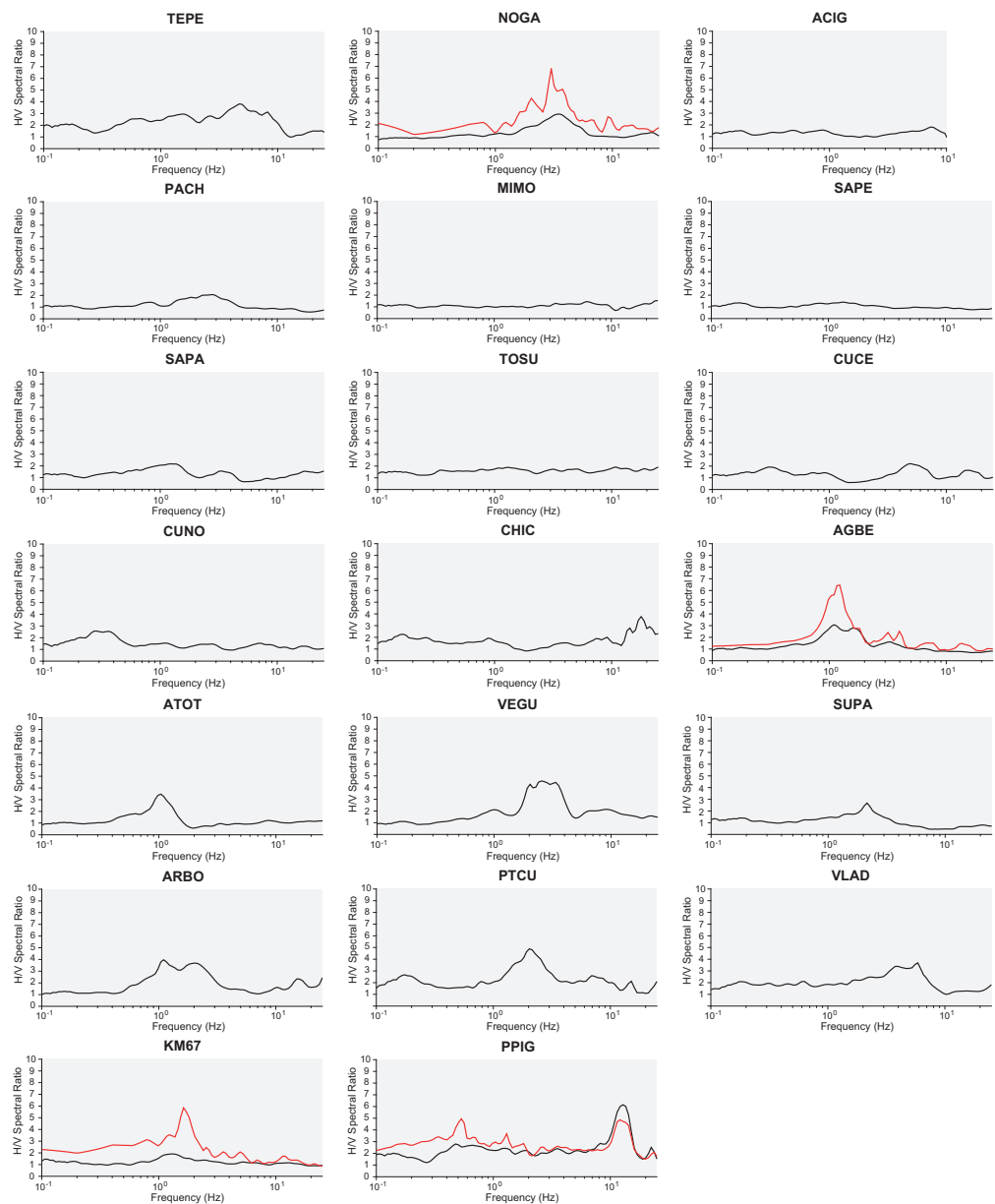


Figure 10. Average HVSR curves for some stations located in the central-eastern sector of the TMVB. Blackline: HVSR results using ambient noise records; redline: HVSR results using earthquake records.

3.4. Eastern TMVB

Regarding relevant historic earthquakes in this sector, it can be mentioned the one occurred in 1546 that caused important damage in the city of Jalapa and nearby towns. There is no specific date reported for this event nor wider descriptions in the historical records, but it is known that the first Catholic church built in America was destroyed [41]. Later, on 4 January 1920 an earthquake with magnitude Mw 6.4 occurred in the city of Jalapa. This event caused structural damage in nearby towns and it seconds the 1985 Michoacán earthquake in terms of fatalities.

Figure 11 shows the seismological stations analyzed in this sector. Most of them belong to the temporary network GECO and only two to the permanent network of the SSN.

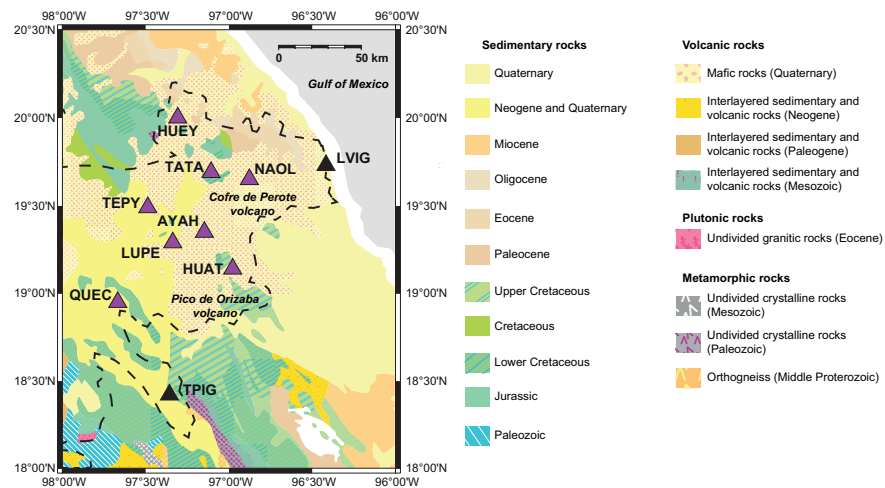


Figure 11. Geological units in the eastern sector of the TMVB [35]. Purple triangles: GECO temporary network stations; black triangles: SSN permanent network stations. Dashed line: TMVB.

In this sector, it was possible to analyze almost half of the stations with earthquake data (Figure 12). In the case of the LVIG station, no significant differences are found between the curves obtained using ambient noise and the ones obtained through earthquake data. As well as in this station, in AYAH and TPIG, no contrast of impedances is observed, and the shape of the curves is almost flat, indicating hard rock sites.

Moreover, TEPEY was located on Quaternary mafic rocks, while QUEEC and LUPE on Neogene and Quaternary sedimentary rocks. In these stations, there are multiple peaks. For station TEPEY it is not possible to identify a value for the resonant frequency. As for QUEEC and LUPE, there is a peak near 10 Hz, which may indicate the presence of thin deposits of sediments. Likewise, the peaks at lower frequencies could be due to the influence of sedimentary rocks from the Neogene and Upper Cretaceous.

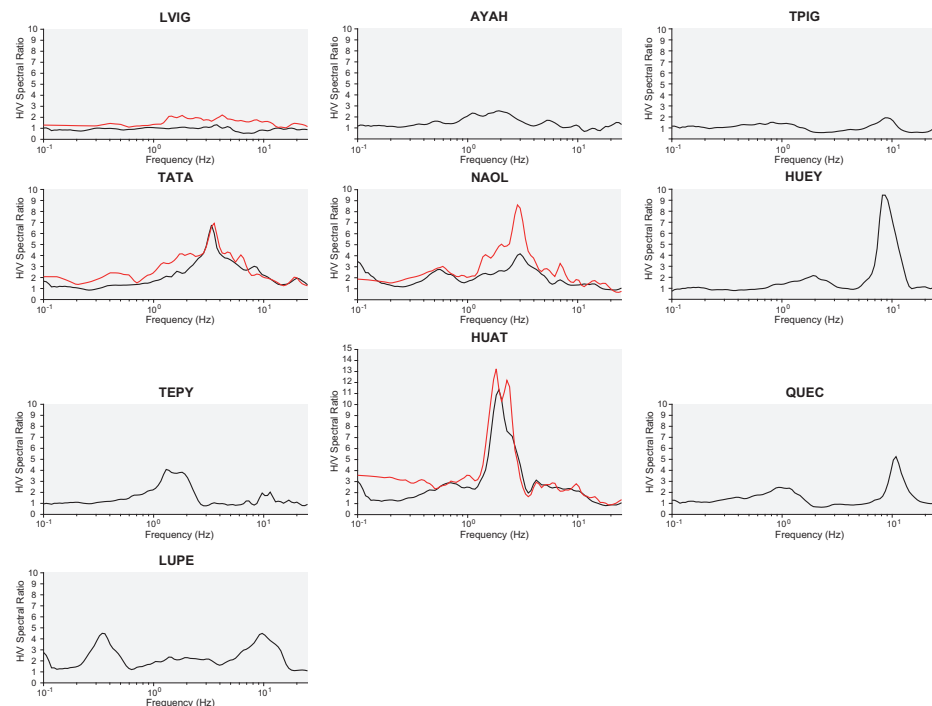


Figure 12. Average HVSR curves for stations located in the Eastern sector of the TMVB. Blackline: HVSR results using ambient noise records; redline: HVSR results using earthquake records.

Stations TATA, NAOL, HUEY, and HUAT are on Quaternary mafic rocks and have varied fundamental frequencies. The observed clear peaks could be attributed to impedance contrasts related to layers of sediments with varied thickness. In TATA and HUAT, there are visible peaks between 1 and 10 Hz. The shape of these curves does not vary significantly when using earthquake and ambient noise data. In the case of the NAOL station, the amplitude of the peak is increased but its location in the considered frequency range does not change.

4. Conclusions

From the results obtained in this study, it is observed that the site response in terms of the fundamental frequency f_0 had a wide variety throughout the TMVB and there was no visible correlation between the shape of the HVSR curves and extent of any particular geological unit. In almost 46% of the stations analyzed, the response was mostly flat or it was not possible to identify clear peaks. In most of these cases, no significant impedance contrasts were observed, so they could be considered as hard rock sites. There was another small group of stations distributed in the four sectors, in which multiple peaks were observed in the HVSR curves. Some of these peaks could be identified as spurious or attributable to the influence of underlying layers of varying stiffness and thickness.

Additionally, in approximately 36% of the analyzed sites there were clear peaks of varied amplitude in the HVSR curves. In these cases, it was possible to identify the value of the resonance frequency, which was mostly between 1 and 10 Hz. Similarly, in some sites there were peaks in frequencies lower than 1 Hz, which should not be underestimated considering the modern trend of tall buildings in the populated areas of the TMVB.

To date, most of the seismicity studies in Mexico have focused on earthquakes originated on the Pacific Ocean coast. Except for Mexico City, due to its geotechnical properties, the amplitude of these events usually reaches the TMVB considerably attenuated. For this reason, this study focused on analyzing what happens in this zone with regional earthquakes. In this regard, it is important to note that there were sites with high peaks in the four sectors analyzed, not only in the central-eastern sector where Mexico City is located.

In some stations, it was possible to make a comparison of the results obtained from ambient noise and earthquake records. In most of them, there were no significant differences in the shape of the average HVSR curves. In the analyses carried out with seismic records, no evidence of non-linear behavior was identified in the site response with respect to the ambient noise results. This could be attributed to the fact that most of the events considered are of low magnitude. In general, there are few major earthquakes with both epicenter and instrumental records inside the TMVB. However, there were some sites with a flat HVSR ambient noise curve in which new peaks appeared when analyzing earthquake data. Considering that the energy associated with ambient noise is not comparable to that associated with a seismic event, it is possible that several sites considered as hard rock may have significant amplifications during the occurrence of an earthquake.

Based on these observations, we consider it is necessary to increase the density of the permanent seismic instrumentation in the TMVB. This will allow to have greater coverage, better quality records, and the possibility of carrying out more analyses using earthquake data, including the SSR technique. A greater permanent seismic instrumentation would allow obtaining isofrequency maps, which could be used in soil-structure interaction analyses and as a basis for estimating seismic hazards and risk assessment in the TMVB. This would also allow to better delimit the risk of populated zones based on local seismicity, considering the significant growth that the cities in the area have had in recent years.

Author Contributions: Conceptualization, L.F.P.-M., Q.R.-P. and F.R.Z.; methodology, L.F.P.-M.; formal analysis, L.F.P.-M.; investigation, L.F.P.-M. and M.A.P.-L.; writing—original draft preparation, L.F.P.-M.; writing—review and editing, Q.R.-P., F.R.Z., J.H.-R. and M.d.l.L.P.-R.; supervision, J.H.-R., M.d.l.L.P.-R. and M.A.P.-L. All authors have read and agreed to the published version of the manuscript.

Funding: This research received no external funding. The APC was funded by L.F.P.-M.

Institutional Review Board Statement: Not applicable.

Informed Consent Statement: Not applicable.

Acknowledgments: Special thanks to the Mexican National Council for Science and Technology (CONACYT) for the support provided to L. Francisco Pérez-Moreno during the realization of his Ph.D. studies and to Quetzalcoatl Rodríguez-Pérez in the Cátedras program (project 1126). SSN data was obtained by the Servicio Sismológico Nacional (México). Station maintenance, data acquisition, and distribution is thanks to its personnel. The authors thank Antonio de J. Mendoza Carvajal and Jorge A. Real Pérez for the maintenance and operation of the Geometry of the Cocos Plate (GECO) array. This network was financed by PAPIIT (projects IN110913, IN105816, and IN106119) and CONACYT (project 177676). We are also particularly grateful to Xyoli Pérez-Campos for providing access to the network data. We appreciate the contributions of the four anonymous reviewers of the initial version of this paper. Their valuable comments allowed us to improve this study.

Conflicts of Interest: The authors declare no conflict of interest.

References

1. Borcherdt, R.D. Effects of local geology on ground motion near San Francisco bay. *Bull. Seismol. Soc. Am.* **1970**, *60*, 29–61.
2. Nakamura, Y. A method for dynamic characteristics estimation of subsurface using microtremor on the ground surface. *Railw. Tech. Res. Inst. Q. Rep.* **1989**, *30*, 25–33.
3. Perron, V.; Gélis, C.; Froment, B.; Hollender, F.; Bard, P.Y.; Cultrera, G.; Cushing, E.M. Can broad-band earthquake site responses be predicted by the ambient noise spectral ratio? Insight from observations at two sedimentary basins. *Geophys. J. Int.* **2018**, *215*, 1442–1454. [[CrossRef](#)]
4. Gosar, A. Study on the applicability of the microtremor HVSR method to support seismic microzonation in the town of Idrija (W Slovenia). *Nat. Hazards Earth Syst. Sci.* **2017**, *17*, 925–937. [[CrossRef](#)]
5. Madiari, C.; Facciorusso, J.; Gargini, E. Numerical Modeling of Seismic Site Effects in a Shallow Alluvial Basin of the Northern Apennines (Italy). *Bull. Seismol. Soc. Am.* **2017**, *107*, 2094–2105. [[CrossRef](#)]
6. Stanko, D.; Gülerce, Z.; Markušić, S.; Šalić, R. Evaluation of the site amplification factors estimated by equivalent linear site response analysis using time series and random vibration theory based approaches. *Soil Dyn. Earthq. Eng.* **2019**, *117*, 16–29. [[CrossRef](#)]
7. Sun, Q.; Guo, X.; Dias, D. Evaluation of the seismic site response in randomized velocity profiles using a statistical model with Monte Carlo simulations. *Comput. Geotech.* **2020**, *120*, 103442. [[CrossRef](#)]
8. Falcone, G.; Romagnoli, G.; Naso, G.; Mori, F.; Peronace, E.; Moscatelli, M. Effect of bedrock stiffness and thickness on numerical simulation of seismic site response. Italian case studies. *Soil Dyn. Earthq. Eng.* **2020**, *139*, 106361. [[CrossRef](#)]
9. Singh, S.K.; Quintanar-Robles, L.; Arroyo, D.; Cruz-Atienza, V.C.; Espíndola, V.H.; Bello-Segura, D.I.; Ordaz, M. Lessons from a Small Local Earthquake (Mw 3.2) That Produced the Highest Acceleration Ever Recorded in Mexico City. *Seismol. Res. Lett.* **2020**, *91*, 3391–3406. [[CrossRef](#)]
10. Ferrari, L.; Orozco-Esquivel, T.; Vlad, C.; Marina, M. The dynamic history of the Trans-Mexican Volcanic Belt and the Mexico subduction zone. *Tectonophysics* **2012**, *522–523*, 122–149. [[CrossRef](#)]
11. Suárez, G.; Caballero-Jiménez, G.V.; Novelo-Casanova, D.A. Active Crustal Deformation in the Trans-Mexican Volcanic Belt as Evidenced by Historical Earthquakes During the Last 450 Years. *Tectonics* **2019**, *38*, 3544–3562. [[CrossRef](#)]
12. Suárez, G.; Ruiz-Barón, D.; Chico-Hernández, C.; Zúñiga, F.R. Catalog of Preinstrumental Earthquakes in Central Mexico: Epicentral and Magnitude Estimations Based on Macroseismic Data. *Bull. Seismol. Soc. Am.* **2020**, *110*, 3021–3036. [[CrossRef](#)]
13. Suter, M.; Carrillo-Martínez, M.; Quintero, O. Macroseismic Study of Shallow Earthquakes in the Central and Eastern Parts of the Trans-Mexican Volcanic Belt, Mexico. *Bull. Seismol. Soc. Am.* **1996**, *86*, 1952–1963.
14. Sahakian, V.J.; Melgar, D.; Quintanar, L.; Ramírez-Guzmán, L.; Pérez-Campos, X.; Baltay, A. Ground motions from the 7 and 19 September 2017 Tehuantepec and Puebla-Morelos, Mexico, earthquakes. *Bull. Seismol. Soc. Am.* **2018**, *108*, 3300–3312. [[CrossRef](#)]
15. Ordaz, M.; Singh, S.K. Source spectra and spectral attenuation of seismic waves from Mexican earthquakes, and evidence of amplification in the hill zone of Mexico City. *Bull. Seismol. Soc. Am.* **1992**, *82*, 24–43.
16. García, D.; Singh, S.K.; Herráiz, M.; Pacheco, J.F.; Ordaz, M. Inslab earthquakes of Central Mexico: Q, source spectra, and stress drop. *Bull. Seismol. Soc. Am.* **2004**, *94*, 789–802. [[CrossRef](#)]
17. Singh, S.K.; Iglesias-Mendoza, A.; García, D.; Pacheco, J.F.; Ordaz, M. Q of Lg waves in the central Mexican Volcanic Belt. *Bull. Seismol. Soc. Am.* **2007**, *97*, 1259–1266. [[CrossRef](#)]
18. Lozano, L.; Herráiz, M.; Singh, S.K. Site effect study in central Mexico using H/V and SSR techniques: Independence of seismic site effects on source characteristics. *Soil Dyn. Earthq. Eng.* **2009**, *29*, 504–516. [[CrossRef](#)]
19. Clemente-Chávez, A.; Zúñiga, F.R.; Lermo, J.; Figueroa-Soto, A.; Valdés-González, C.; Montiel, M.; Chávez, O.; Arroyo, M. On the behavior of site effects in central Mexico (the Mexican volcanic belt-MVB), based on records of shallow earthquakes that occurred in the zone between 1998 and 2011. *Nat. Hazards Earth Syst. Sci.* **2014**, *14*, 1391–1406. [[CrossRef](#)]

20. Zúñiga, F.R.; Lacan, P.; Rodríguez-Pérez, Q.; Márquez-Ramírez, V.H. Temporal and spatial evolution of instrumented seismicity in the Trans-Mexican Volcanic Belt. *J. S. Am. Earth Sci.* **2020**, *98*, 102390. [[CrossRef](#)]
21. Ruggieri, S.; Tosto, C.; Rosati, G.; Uva, G.; Ferro, G.A. Seismic Vulnerability Analysis of Masonry Churches in Piemonte after 2003 Valle Scrivia Earthquake: Post-event Screening and Situation 17 Years Later. *Int. J. Archit. Herit.* **2020**, 1–29. [[CrossRef](#)]
22. Godínez-Domínguez, E.A.; Tena-Colunga, A.; Pérez-Rocha, L.E.; Archundia-Aranda, H.I.; Gómez-Bernal, A.; Ruiz-Torres, R.P.; Escamilla-Cruz, J.L. The September 7, 2017 Tehuantepec, Mexico, earthquake: Damage assessment in masonry structures for housing. *Int. J. Disaster Risk Reduct.* **2021**, *56*, 1–29. [[CrossRef](#)]
23. Catálogo de Sismos. Available online: <http://www2.ssn.unam.mx:8080/catalogo/> (accessed on 16 October 2020).
24. Search Earthquake Catalog. Available online: <https://earthquake.usgs.gov/earthquakes/search/> (accessed on 16 October 2020).
25. ISC Bulletin: Event Catalogue Search. Available online: <http://www.isc.ac.uk/iscbulletin/search/catalogue/> (accessed on 16 October 2020).
26. GEOSCOPE. *French Global Network of Broad Band Seismic Stations*; Institut de Physique du Globe de Paris (IPGP) and Ecole Et Observatoire Des Sciences De La Terre De Strasbourg (EOST). [[CrossRef](#)]
27. Meso America Subduction Experiment. Caltech. Dataset. [[CrossRef](#)]
28. Pérez-Campos, X. MASE: Undergraduate Research and Outreach as Part of a Large Project. *Seismol. Res. Lett.* **2008**, *92*, 232–236. [[CrossRef](#)]
29. West, M. The Colima Deep Seismic Experiment: Imaging the Magmatic Root of Colima Volcano. *Int. Fed. Digit. Seismogr. Netw.* **2006**.
30. Yang, T.; Grand, S.P.; Wilson, D.; Guzman-Speziale, M.; Gomez-Gonzalez, J.M.; Dominguez-Reyes, T. Seismic structure beneath the Rivera subduction zone from finite-frequency seismic tomography. *J. Geophys. Res. Solid Earth* **2009**, *114*, B01302. [[CrossRef](#)]
31. Rodríguez-Domínguez, M.; Pérez-Campos, X.; Montealegre-Cázares, C.; Clayton, R.W.; Cabral-Cano, E. Crustal structure variations in south-central Mexico from receiver functions. *Geophys. J. Int.* **2019**, *219*, 2174–2186. [[CrossRef](#)]
32. Wathelet, M.; Chatelain, J.L.; Cornou, C.; Giulio, G.D.; Guillier, B.; Ohrnberger, M.; Savvaidis, A. Geopsy: A user-friendly open-source tool set for ambient vibration processing. *Seismol. Res. Lett.* **2020**, *91*, 1878–1889. [[CrossRef](#)]
33. Konno, K.; Ohmachi, T. Ground-motion characteristics estimated from spectral ratio between horizontal and vertical components of microtremor. *Bull. Seismol. Soc. Am.* **1998**, *88*, 228–241.
34. SESAME Team. *Guidelines for the Implementation of the H/V Spectral Ratio Technique on Ambient Vibrations: Measurements, Processing and Interpretation*; SESAME European Research Project. 2004. Available online: http://sesame.geopsy.org/Papers/HV_User_Guidelines.pdf (accessed on 15 August 2020).
35. Reed, J.C.; Wheeler, J.O.; Tucholke, B.E. *Decade of North American Geology Geologic Map of North America—Perspectives and Explanation*; The Geological Society of America: Boulder, CO, USA, 2015.
36. Suter, M. The A.D. 1567 Mw 7.2 Ameca, Jalisco, Earthquake (Western Trans-Mexican Volcanic Belt): Surface Rupture Parameters, Seismogeological Effects, and Macroseismic Intensities from Historical Source. *Bull. Seismol. Soc. Am.* **2015**, *105*, 646–656. [[CrossRef](#)]
37. Suter, M. The 1563 MI 8 Puerto de la Navidad Subduction-Zone and 1567 Mw 7.2 Ameca Crustal Earthquakes (Western Mexico): New Insights from Sixteenth-Century Sources. *Seismol. Res. Lett.* **2019**, *90*, 366–375. [[CrossRef](#)]
38. Suter, M. The 2 October 1847 MI 5.7 Chapala Graben Triggered Earthquake (Trans-Mexican Volcanic Belt, West-Central Mexico): Macroseismic Observations and Hazard Implications. *Seismol. Res. Lett.* **2017**, *89*, 35–46. [[CrossRef](#)]
39. Lacan, P.; Aguirre-Díaz, G.; Audin, L.; Perea, H.; Baize, S.; Zúñiga, F.R.; Ortuño, M. Sedimentary evidence of historical and prehistorical earthquakes along the Venta de Bravo Fault System, Acambay Graben (Central Mexico). *Sediment. Geol.* **2018**, *365*, 62–77. [[CrossRef](#)]
40. Rodríguez-Pérez, Q.; Zúñiga, F.R. Seismicity characterization of the Maravatío-Acambay and Actopan regions, central Mexico. *J. S. Am. Earth Sci.* **2017**, *76*, 264–275. [[CrossRef](#)]
41. Suárez, G.; Novelo-Casanova, D.A. A Pioneering Aftershock Study of the Destructive 4 January 1920 Jalapa, Mexico, Earthquake. *Seismol. Res. Lett.* **2018**, *89*, 1894–1899. [[CrossRef](#)]